CHINESE OPTICS LETTERS

Vol. 21, No. 9 | September 2023

2 kW random fiber laser based on hybrid Yb-Raman gain [Invited]

Jun Ye (叶 俊)[1,2,3], Yang Zhang (张 扬)[1], Junrui Liang (梁峻锐)[1], Xiaoya Ma (马小雅)[1], Jiangming Xu (许将明)[1*], Tianfu Yao (姚天甫)[1,2,3], Jinyong Leng (冷进勇)[1,2,3], and Pu Zhou (周 朴)[1**]

[1] College of Advanced Interdisciplinary Studies, National University of Defense Technology, Changsha 410073, China

[2] Nanhu Laser Laboratory, National University of Defense Technology, Changsha 410073, China

[3] Hunan Provincial Key Laboratory of High Energy Laser Technology, National University of Defense Technology, Changsha 410073, China

*Corresponding author: jmxu1988@163.com

**Corresponding author: zhoupu203@163.com

Received May 1, 2023 | Accepted June 26, 2023 | Posted Online August 18, 2023

High-power operation is one of the most important research topics surrounding random fiber lasers (RDFLs). Here we optimized the cavity structure and proposed a new scheme based on hybrid gain to address the issue of high-power backward light in traditional kilowatt-level RDFLs. Consequently, a record power of 1972 W was achieved while the maximum backward leaked power only reached 0.12 W. The conversion efficiency relative to the laser diode pump power was 68.4%, and the highest spectral purity of the random lasing reached 98.1%. This work may provide a reference for high-power RDFLs, Raman fiber lasers, and long-wavelength Yb-doped fiber lasers.

Keywords: random fiber laser; high power; hybrid gain; stimulated Raman scattering; Rayleigh scattering.

DOI: 10.3788/COL202321.090004

1. Introduction

Conventional fiber lasers generate lasing output through feedback between two mirrors at either end of the laser cavity. In contrast, random fiber lasers (RDFLs) utilize random distributed feedback enabled by Rayleigh backscattering[1], which allows for a simplified structure, no longitudinal modes, and emission at any wavelength through cascaded Raman processes[2,3]. RDFLs have attracted much attention in recent years due to their distinctive operating principle. Existing research on RDFLs can be categorized into topics such as power/brightness enhancement[4–7], spectral manipulation[8–10], temporal modulation[11,12], and transverse mode control[13,14]. These advances have led to practical applications of RDFLs in sensing[15–17], communication[18,19], imaging[20,21], and nonlinear frequency conversion[22,23].

One of the main research topics concerning RDFLs is high-power operation. On the one hand, an RDFL can serve as a robust seed for high-power fiber amplifiers[5,24–26]; on the other hand, it can directly achieve high-power output[4,27–29]. Early RDFLs relied on several or even tens of kilometers of passive fiber to provide sufficient distributed feedback[30], thus enabling low-threshold random lasing output. However, the use of such long passive fiber also reduced the threshold of second-order Stokes waves, thereby limiting the output power of early RDFLs to the watt level[31].

Since 2013, the output power of single-stage RDFLs has rapidly increased by implementing several techniques, which include replacing full-opened cavities with half-opened structures[27], shortening the length of passive fiber[32], increasing the mode field area[28], reducing the number of fiber modes (appropriately reducing the numerical aperture of the fiber core)[29], and adopting a more temporally stable pump source[4]. Thanks to these techniques, high-power output of up to 1.57 kW was achieved in 2021[4]. However, further power scaling faces numerous challenges. For example, in the first kilowatt-level RDFL, the optical spectrum broadened dramatically during the power scaling process, exceeding the reflection bandwidth of the highly reflective fiber Bragg grating (FBG). As a result, a maximum backward output power of up to 66 W was observed at the highest pump power[29]. Subsequently, Song *et al*. utilized a phase-modulated single-frequency fiber laser as the pump source and achieved a high-power random lasing output of 1570 W with 77.5% conversion efficiency and the highest spectral purity of 92.4%. However, as output signal power increased above 678 W, the spectrum broadened rapidly and exceeded the reflection bandwidth of the highly reflective FBG, resulting in a maximum backward output power of 40.2 W at the highest pump power[4]. Therefore, the generation of high-power backward light assisted by spectral broadening has become a new obstacle limiting the power scaling of single-stage RDFLs.

In this Letter, we optimized the cavity structure of high-power RDFLs, and proposed a new scheme based on hybrid Yb-Raman gain to address the issue of high-power backward light in traditional kilowatt-level RDFLs, further boosting the output power to 2-kW level. This work may provide a reference not only for high-power RDFLs, but also for Raman fiber lasers and long-wavelength Yb-doped fiber lasers.

2. Theoretical Analysis

First, it is necessary to clarify the physical mechanism of high-power backward light generation in traditional high-power RDFLs. Without loss of generality, a half-opened RDFL pumped by an Yb-doped fiber amplifier is considered as the typical structure, as shown in Fig. 1(a). The pump seed is injected into the main amplifier through a circulator, and after the pump stage, a highly reflective FBG and a section of Ge-doped fiber (GDF) are spliced to form a half-opened RDFL. The high-power random lasing is ultimately output to free space using a quartz block head (QBH). A generalized nonlinear Schrödinger equation model and a steady-state rate equation model are utilized to simulate the RDFL and the pump source's main amplifier, respectively[33]. The pump wavelength is set at 1075 nm, and the pump power is 1300 W. The maximum reflectivity of the FBG is set to 99%, the center wavelength is 1130 nm, the reflection bandwidth is 4 nm, and the shape of the reflection spectrum is approximated by a second-order hyper-Gaussian function. The reflectivity of the QBH is set to 2×10^{-5}, and the core and cladding diameters of the fibers are 20 and 400 μm, respectively.

At the maximum output power (1036 W), the optical spectrum of the random lasing exhibits substantial broadening such that a portion of light leaks from the FBG and injects into the main amplifier of the pump source. Figure 1(c) shows the simulated leaked optical spectrum. Due to the reflection effect of the FBG, the leaked optical spectrum shows a significant dip at 1130 nm, and the total leaked power reaches 1.31 W. Additionally, the effective reflectivity of the FBG decreases to 75.2% (recall that the nominal reflectivity is 99%). Although the leaked power may seem small when compared to the kilowatt-level output, it can be amplified significantly when injecting into the pump source's main amplifier. As can be seen in Fig. 1(b), the 1.31 W leaked light can be amplified to 44.5 W and evolves into a powerful backward output. We have numerically verified that this issue is unavoidable in traditional high-power RDFLs. Therefore, optimizing the system structure is of utmost importance.

Given that the amplification of FBG leakage by the pump source is inevitable, we propose incorporating the main amplifier of the pump source into the RDFL, as illustrated in Fig. 2(a). By moving the highly reflective FBG before the main amplifier of the pump source, this structure combines Raman gain and doping ion gain and is referred to as an "RDFL based on hybrid gain." Although previous reports have attempted to use hybrid gain in RDFLs[34,35], this approach has only achieved output powers in the watt level and has never been applied in high-power RDFLs at the kilowatt level.

To investigate the power characteristics of hybrid-gain RDFLs, we established a theoretical model by considering stimulated Raman scattering and Rayleigh backscattering in the steady-state rate equations, which can be written as

$$\pm\frac{\mathrm{d}P_d^{\pm}}{dz} = \{-\Gamma_d[\sigma_{ad}N_0 - (\sigma_{ad} + \sigma_{ed})N_2] - \alpha_d\}P_d^{\pm}, \tag{1}$$

$$\frac{\mathrm{d}P_p^{+}}{\mathrm{d}z} = \{\Gamma_p[(\sigma_{ap} + \sigma_{ep})N_2 - \sigma_{ap}N_0] - \alpha_p\}P_p^{+} - \frac{\lambda_r}{\lambda_p}g_R(P_r^{+} + P_r^{-} + 4h\nu_r\Delta\nu_r B_r)P_p^{+}, \tag{2}$$

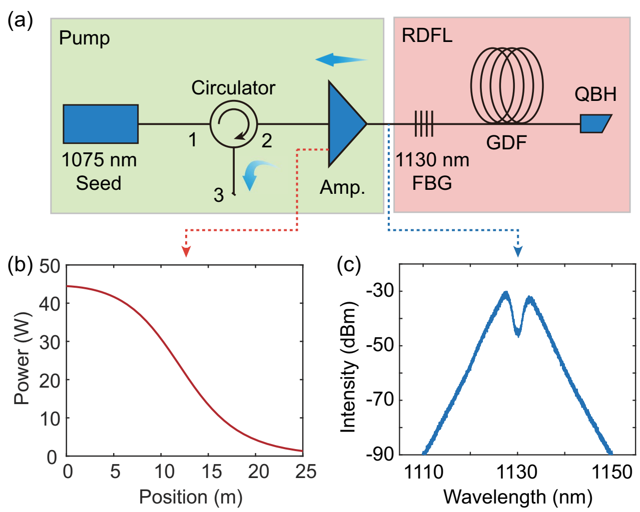

Fig. 1. (a) Typical structure of traditional high-power RDFLs; (b) power amplification of backward-leaked random lasing in pump source's main amplifier; (c) optical spectrum of the leaked random lasing.

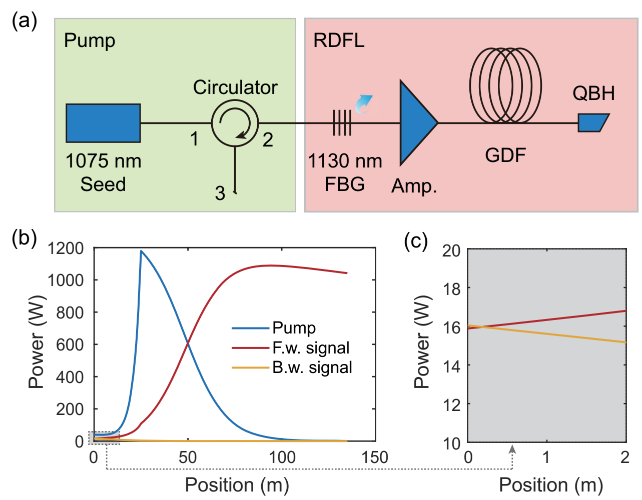

Fig. 2. (a) Schematic of an RDFL based on hybrid Yb-Raman gain; (b) longitudinal power distribution (F.w., forward; B.w., backward); (c) zoom-in of the longitudinal power distribution near the 1130 nm FBG.

$$\pm\frac{\mathrm{d}P_r^{\pm}}{\mathrm{d}z}=\{\Gamma_r[(\sigma_{ar}+\sigma_{er})N_2-\sigma_{ar}N_0]-\alpha_r\}P_r^{\pm} + g_R P_p^{+}(P_r^{\pm}+2h\nu_r\Delta\nu_r B_r)+\varepsilon_r P_r^{\mp}, \tag{3}$$

$$\frac{N_2}{N_0}=\frac{\sum_{k=d,p,r}[P_k^{+}(z)+P_k^{-}(z)]\sigma_{ak}\Gamma_k\lambda_k}{\sum_{k=d,p,r}[P_k^{+}(z)+P_k^{-}(z)](\sigma_{ak}+\sigma_{ek})\Gamma_k\lambda_k+\frac{hcA_c}{\tau}}, \tag{4}$$

where the subscripts d, p, and r represent the laser diode (LD) pump light, Raman pump light, and random lasing, respectively. P^+ and P^- stand for the optical power in the forward and backward directions. Γ is the overlap factor, and σ_a and σ_e are the absorption and emission cross sections, respectively. α denotes the attenuation coefficient. g_R is the Raman gain coefficient, and ε stands for the Rayleigh backscattering coefficient. h is the Planck constant, and c is the speed of light in vacuum. N_2 denotes the number of excited Yb ions, and N_0 represents the dopant concentration. A_c is the doped cross-sectional area, and τ is the upper-level lifetime of the gain medium. Additionally, the boundary conditions can be written as

$$P_d^{+}(0)=P_{dL}, \tag{5}$$

$$P_d^{-}(L_1)=P_{dR}, \tag{6}$$

$$P_p^{+}(0)=P_{p\_seed}, \tag{7}$$

$$P_r^{+}(0)=R_L P_r^{-}(0), \tag{8}$$

$$P_r^{-}(L)=R_R P_r^{+}(L), \tag{9}$$

where P_{dL} and P_{dR} refer to the forward and backward powers of the LD pump light, P_{p_seed} represents the seed power of Raman pump light, which is set to 40 W in this example. L_1 and L signify the length of the Yb-doped fiber (YDF) and the total fiber length, respectively. R_L and R_R denote the reflectivity of the highly reflective FBG and that of the QBH, respectively. A modified relaxation algorithm is utilized for the numerical simulation; the parameter values used in the calculations are shown in Table 1.

Table 1. Parameter Values in the Simulation.

Symbol	Value
Γ_d, Γ_p, Γ_r	0.0025, 0.85, 0.85
α_d, α_p, α_r	$(1.55, 1.5, 1.45)\times10^{-3}$ m^{-1}
λ_d, λ_p, λ_r	976, 1075, 1130 nm
L_1, L	25, 135 m
$\Delta\nu_r$	0.25 THz
g_R	0.075 W^{-1}/km
ε_r	2.55×10^{-6}
A_c	3.14×10^{-10} m^2
N_0	4.557×10^{25} m^{-1}
R_L, R_R	0.99, 2×10^{-5}

Figure 2(b) shows the longitudinal power distribution at an LD pump power of 1400 W. The results indicate that the 1075 nm Raman pump light is rapidly amplified in a 25 m-long YDF, with a maximum power of approximately 1179 W. The power of the 1130 nm random lasing reaches 109 W at the connection point between the YDF and the passive fiber, and subsequently increases rapidly due to the effect of Raman gain, ultimately reaching 1041 W at the output end. Additionally, Fig. 2(c) highlights that the power of the random lasing at the highly reflective FBG is approximately 16 W, and the power of the FBG leakage is only 0.16 W, indicating that the hybrid-gain RDFL can effectively suppress the generation of high-power backward lasing.

3. Experimental Setup

Based on the theoretical design, a hybrid-gain half-opened RDFL is constructed, as depicted in Fig. 3. Previous reports have shown that a temporally stable pump source is of great importance for high-performance RDFLs[36–38]; therefore, a superfluorescent fiber source (SFS) with customizable optical spectrum is used as the Raman pump seed[39], providing an output power of about 40 W. To extract the backward FBG leakage, a 10/125 μm circulator is spliced after the SFS. Subsequently, a mode field adapter (MFA) with input and output fiber dimensions of 10/125 μm and 20/400 μm, respectively, is then connected after the circulator. A 20/400 μm highly reflective FBG with a 2.78 nm reflection bandwidth and a reflectivity of about 99% is used to provide point feedback. The hybrid gain and random distributed feedback are provided by a 25 m-long 20/400 μm YDF and a section of 20/400 μm GDF. A backward

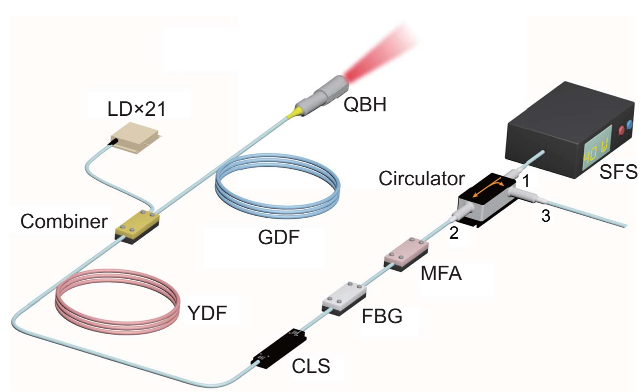

Fig. 3. Experimental setup of the RDFL based on hybrid Yb-Raman gain. LD, laser diode; YDF, Yb-doped fiber; GDF, Ge-doped fiber; QBH, quartz block head; CLS, cladding light stripper; FBG, fiber Bragg grating; MFA, mode field adaptor; SFS, superfluorescent fiber source.

pump structure is employed in the active-gain stage, which consists of 21 LDs with a maximum pump power of more than 3 kW. Additionally, to filter out the residual LD pump light, a cladding light stripper (CLS) is spliced between the FBG and the YDF. Finally, a QBH is used to output the high-power random lasing to free space.

4. Results and Discussion

We found in a previous investigation that a relatively broad pump bandwidth can help suppress spectral broadening and achieve a high output power while maintaining a high spectral purity[40]. Similarly, here the pump bandwidth is optimized to 12 nm, and the GDF is shortened to 25 m for suppressing the second-order Stokes wave. However, taking into account the pigtails of the combiner and the QBH, the passive fiber has a total length of 35 m; thus the whole "cavity length" of the RDFL reaches 60 m. We first investigated the spectral characteristics of the hybrid-gain RDFL. Figure 4(a) shows the output spectrum with the highest spectral purity of the signal light. At this point, the LD pump power is about 2789 W, and the spectral purity of the signal light reaches as high as 98.1%, which is the highest spectral purity among kilowatt-level RDFLs, to the best of our knowledge. Meanwhile, the intensity difference between the signal and the residual Raman pump wave is about 20.2 dB, and the suppression ratio of the second-order Stokes wave is about 34.1 dB. Figure 4(b) demonstrates the evolution of the signal's root-mean-square (RMS) linewidth with the LD pump power. The results reveal that, as the LD pump power increases, the RMS linewidth of the signal light broadens linearly from 2.1 nm near the threshold to 6.7 nm at the maximum output power.

The power evolution of each spectral component is shown in Fig. 5(a). The result indicates that the lasing threshold is about 1460 W. At an LD pump power of 2881 W, the maximum output power of the signal light reaches 1972 W, with a corresponding conversion efficiency of 68.4%. Since the conversion efficiency reported here is relative to the LD pump power, it is higher than the conversion efficiency reported for previously developed kilowatt-level RDFLs[4,29]. Moreover, the second-order Stokes power is only 0.7 W at the highest output power. Figure 5(b) shows the evolution of the backward-leaked power (measured

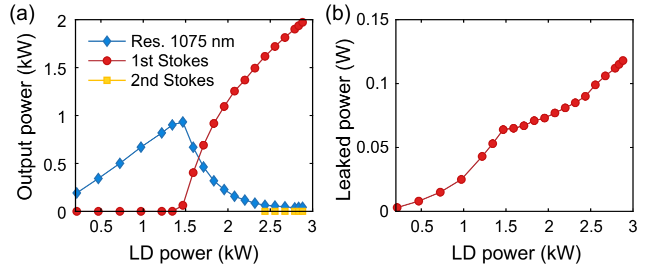

Fig. 5. (a) Power evolutions of residual 1075 nm pump wave, forward first-order Stokes wave (random lasing), and second-order Stokes wave; (b) power of backward-leaked random lasing as a function of LD power.

at the third port of the circulator) with the LD pump power. The nonlinear evolution of the backward-leaked power can be divided into two regions, which are separated by the lasing threshold. Below the threshold, the backward-leaked power grows rapidly, mainly as a result of the backward scattering of the 1075 nm Raman pump light. Above the threshold, the 1075 nm Raman pump light is converted into 1130 nm random lasing, causing the growth of the backward-leaked power to gradually slow down. Consequently, at the LD pump power of 2881 W, the maximum backward-leaked power is only 0.12 W.

To verify that the output lasing is generated by an RDFL instead of a fiber oscillator, the temporal characteristics of the output are measured. Figure 6(a) shows the normalized temporal profile at the maximum output power, which is highly stable under a measurement bandwidth of 20 MHz, with a normalized standard deviation (NSTD) of only 0.48%. Figure 6(b) shows the radio-frequency (RF) spectrum of the temporal profile, revealing that there is no characteristic frequency corresponding to the cavity length (i.e., $c/2nL \sim 1.72\,\mathrm{MHz}$). It should be noted that the two peaks (0.32 and 0.39 MHz) in the RF spectrum result from the intensity noise of the Raman pump source (i.e., the SFS), and do not indicate the presence of longitudinal modes in the developed RDFL. In order to confirm this, we experimentally measured the temporal profile and the corresponding RF spectrum of the SFS, and verified the existence of the two characteristic frequencies.

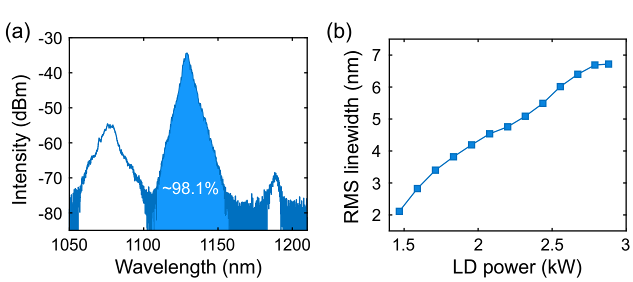

Fig. 4. (a) Output spectrum with the highest spectral purity; (b) RMS spectral linewidth of the random lasing as a function of LD power.

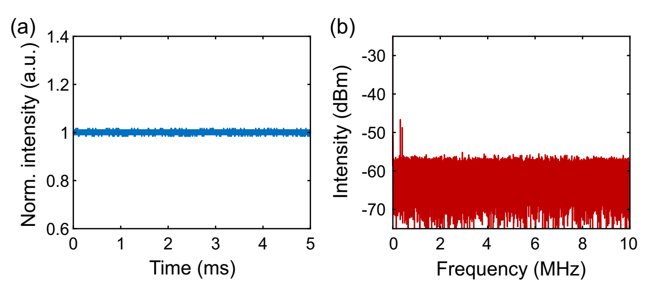

Fig. 6. (a) Temporal profile of the random lasing at the maximum output power; (b) corresponding RF spectrum.

5. Conclusion

In summary, by optimizing the cavity structure and employing a broadband SFS as the Raman pump source, we achieved a 2-kW hybrid Yb-Raman gain-based RDFL. First, we theoretically revealed that the high-power backward output in traditional high-power RDFLs resulted from the amplification of FBG leakage by the pump source. Subsequently, we established a theoretical model to optimize the cavity structure and proposed a new scheme based on hybrid Yb-Raman gain. Ultimately, a high-power RDFL with a maximum power of 1972 W was obtained. To the best of our knowledge, this is the highest output power reported for RDFLs to date. The conversion efficiency relative to the LD pump power was about 68.4%, which is comparable to that of conventional fiber oscillators operating at 1 μm. Additionally, the maximum backward power was only 0.12 W, demonstrating excellent suppression of high-power backward output. Furthermore, the highest spectral purity of the random lasing reached 98.1%, which is also the highest reported spectral purity to date for kilowatt-level RDFLs.

Acknowledgement

This work was supported in part by the National Natural Science Foundation of China (NSFC) (Nos. 61635005 and 61905284) and the National Postdoctoral Program for Innovative Talents (No. BX20190063).

References

1. S. K. Turitsyn, S. A. Babin, A. E. El-Taher, P. Harper, D. V. Churkin, S. I. Kablukov, J. D. Ania-Castañón, V. Karalekas, and E. V. Podivilov, "Random distributed feedback fibre laser," Nat. Photonics **4**, 231 (2010).
2. D. V. Churkin, S. Sugavanam, I. D. Vatnik, Z. Wang, E. V. Podivilov, S. A. Babin, Y. Rao, and S. K. Turitsyn, "Recent advances in fundamentals and applications of random fiber lasers," Adv. Opt. Photonics **7**, 516 (2015).
3. A. S. L. Gomes, A. L. Moura, C. B. de Araújo, and E. P. Raposo, "Recent advances and applications of random lasers and random fiber lasers," Prog. Quant. Electron. **78**, 100343 (2021).
4. J. Song, S. Ren, W. Liu, W. Li, H. Wu, P. Ma, H. Zhang, and P. Zhou, "Temporally stable fiber amplifier pumped random distributed feedback Raman fiber laser with record output power," Opt. Lett. **46**, 5031 (2021).
5. T. Qi, D. Li, G. Fu, Y. Yang, G. Li, L. Wang, S. Du, P. Yan, M. Gong, and Q. Xiao, "Amplification of random lasing enables a 10-kW-level high-spectral-purity Yb–Raman fiber laser," Opt. Lett. **48**, 1794 (2023).
6. S. A. Babin, E. I. Dontsova, and S. I. Kablukov, "Random fiber laser directly pumped by a high-power laser diode," Opt. Lett. **38**, 3301 (2013).
7. Y. Chen, C. Fan, T. Yao, H. Xiao, J. Leng, P. Zhou, I. N. Nemov, A. G. Kuznetsov, and S. A. Babin, "Brightness enhancement in random Raman fiber laser based on a graded-index fiber with high-power multimode pumping," Opt. Lett. **46**, 1185 (2021).
8. L. Zhang, Z. Qiu, Z. Xiao, J. Zhang, F. Pang, T. Wang, and X. Bao, "Frequency-stabilized Brillouin random fiber laser enabled by self-inscribed transient population grating," Opt. Lett. **47**, 150 (2022).
9. L. Zhang, J. Dong, and Y. Feng, "High-power and high-order random Raman fiber lasers," IEEE J. Sel. Top. Quantum Electron. **24**, 1400106 (2018).
10. P. Huang, X. Shu, and Z. Zhang, "Multi-wavelength random fiber laser with switchable wavelength interval," Opt. Express **28**, 28686 (2020).
11. J. Xu, J. Ye, W. Liu, J. Wu, H. Zhang, L. Jinyong, and P. Zhou, "Passively spatiotemporal gain-modulation-induced stable pulsing operation of a random fiber laser," Photon. Res. **5**, 598 (2017).
12. W. Pan, L. Zhang, H. Jiang, X. Yang, S. Cui, and Y. Feng, "Ultrafast Raman fiber laser with random distributed feedback," Laser Photonics Rev. **12**, 1700326 (2018).
13. X. Ma, J. Ye, Y. Zhang, J. Xu, J. Wu, T. Yao, J. Leng, and P. Zhou, "Vortex random fiber laser with controllable orbital angular momentum mode," Photon. Res. **9**, 266 (2021).
14. R. Ma, H. H. Zhang, E. Manuylovich, S. Sugavanam, H. Wu, W. L. Zhang, V. Dvoyrin, T. P. Hu, Z. J. Hu, Y. J. Rao, and S. K. Turitsyn, "Tailoring of spatial coherence in a multimode fiber by selectively exciting groups of eigenmodes," Opt. Express **28**, 20587 (2020).
15. B. Han, H. Wu, Y. Liu, S. Dong, Y. Rao, Z. Wang, J. Xu, and L. Ma, "Ultralong single-ended random fiber laser and sensor," Laser Photonics Rev. **17**, 2200797 (2023).
16. D. Leandro, V. DeMiguel-Soto, and M. Lopez-Amo, "High-resolution sensor system using a random distributed feedback fiber laser," J. Lightwave Technol. **34**, 4596 (2016).
17. J. Deng, D. V. Churkin, Z. Xu, and X. Shu, "Random fiber laser based on a partial-reflection random fiber grating for high temperature sensing," Opt. Lett. **46**, 957 (2021).
18. G. Rizzelli, P. Rosa, P. Corredera, and J. D. Ania-Castanon, "Transmission span optimization in fiber systems with cavity and random distributed feedback ultralong Raman laser amplification," J. Lightwave Technol. **35**, 4967 (2017).
19. M. Tan, P. Rosa, S. T. Le, M. A. Iqbal, I. D. Phillips, and P. Harper, "Transmission performance improvement using random DFB laser based Raman amplification and bidirectional second-order pumping," Opt. Express **24**, 2215 (2016).
20. H. Wu, B. Han, Z. Wang, G. Genty, G. Feng, and H. Liang, "Temporal ghost imaging with random fiber lasers," Opt. Express **28**, 9957 (2020).
21. R. Ma, Y. J. Rao, W. L. Zhang, and B. Hu, "Multimode random fiber laser for speckle-free imaging," IEEE J. Sel. Top. Quantum Electron. **25**, 0900106 (2019).
22. E. I. Dontsova, S. I. Kablukov, I. D. Vatnik, and S. A. Babin, "Frequency doubling of Raman fiber lasers with random distributed feedback," Opt. Lett. **41**, 1439 (2016).
23. S. Cui, J. Qian, X. Zeng, X. Cheng, X. Gu, and Y. Feng, "A watt-level yellow random laser via single-pass frequency doubling of a random Raman fiber laser," Opt. Fiber Technol. **64**, 102552 (2021).
24. J. Zhang, G. Bai, X. Li, Y. Yang, B. He, and J. Zhou, "1.36-kW spectral-narrowing fiber laser seeded by random fiber laser," IEEE Photon. Technol. Lett. **31**, 1343 (2019).
25. J. Xu, J. Ye, P. Zhou, J. Leng, H. Xiao, H. Zhang, J. Wu, and J. Chen, "Tandem pumping architecture enabled high power random fiber laser with near-diffraction-limited beam quality," Sci. China Tech. Sci. **62**, 80 (2019).
26. T. Li, Y. Li, W. Ke, C. Zha, W. Peng, Y. Sun, and Y. Ma, "Power scaling of narrow-linewidth fiber amplifier seeded by Yb-doped random fiber laser," IEEE J. Sel. Top. Quantum Electron. **24**, 903208 (2018).
27. H. Zhang, P. Zhou, X. Wang, X. Du, H. Xiao, and X. Xu, "Hundred-watt-level high power random distributed feedback Raman fiber laser at 1150 nm and its application in mid-infrared laser generation," Opt. Express **23**, 17138 (2015).
28. H. Zhang, L. Huang, P. Zhou, X. Wang, J. Xu, and X. Xu, "More than 400 W random fiber laser with excellent beam quality," Opt. Lett. **42**, 3347 (2017).
29. H. Zhang, L. Huang, J. Song, H. Wu, P. Zhou, X. Wang, J. Wu, J. Xu, Z. Wang, X. Xu, and Y. Rao, "Quasi-kilowatt random fiber laser," Opt. Lett. **44**, 2613 (2019).
30. D. V. Churkin, S. A. Babin, A. E. El-Taher, P. Harper, S. I. Kablukov, V. Karalekas, J. D. Ania Castañón, E. V. Podivilov, and S. K. Turitsyn, "Raman fiber lasers with a random distributed feedback based on Rayleigh scattering," Phys. Rev. A **82**, 33828 (2010).
31. I. D. Vatnik, D. V. Churkin, and S. A. Babin, "Power optimization of random distributed feedback fiber lasers," Opt. Express **20**, 28033 (2012).
32. Z. Wang, H. Wu, M. Fan, L. Zhang, Y. Rao, W. Zhang, and X. Jia, "High power random fiber laser with short cavity length: theoretical and experimental investigations," IEEE J. Sel. Top. Quantum Electron. **21**, 10 (2015).

33. J. Ye, X. Ma, Y. Zhang, J. Xu, H. Zhang, T. Yao, J. Leng, and P. Zhou, "Revealing the dynamics of intensity fluctuation transfer in random Raman fiber laser," Photon. Res. **10**, 618 (2022).
34. N. Mohd Yusoff, N. H. Zainol Abidin, M. H. Abu Bakar, M. A. W. Abdul Hadi, and M. A. Mahdi, "Spectral behaviour of hybrid Raman-erbium random fiber laser with dual pumping," Optik **208**, 164535 (2020).
35. H. Wu, Z. Wang, W. Sun, Q. He, Z. Wei, and Y. Rao, "1.5 μm low threshold, high efficiency random fiber laser with hybrid erbium–Raman gain," J. Lightwave Technol. **36**, 844 (2018).
36. J. Xu, Z. Lou, J. Ye, J. Wu, J. Leng, H. Xiao, H. Zhang, and P. Zhou, "Incoherently pumped high-power linearly-polarized single-mode random fiber laser: experimental investigations and theoretical prospects," Opt. Express **25**, 5609 (2017).
37. J. Dong, L. Zhang, H. Jiang, X. Yang, W. Pan, S. Cui, X. Gu, and Y. Feng, "High order cascaded Raman random fiber laser with high spectral purity," Opt. Express **26**, 5275 (2018).
38. V. Balaswamy, S. Ramachandran, and V. R. Supradeepa, "High-power, cascaded random Raman fiber laser with near complete conversion over wide wavelength and power tuning," Opt. Express **27**, 9725 (2019).
39. J. Ye, J. Xu, Y. Zhang, J. Song, J. Leng, and P. Zhou, "Spectrum-manipulable hundred-watt-level high-power superfluorescent fiber source," J. Lightwave Technol. **37**, 3113 (2019).
40. J. Ye, J. Xu, J. Song, Y. Zhang, H. Zhang, H. Xiao, J. Leng, and P. Zhou, "Pump scheme optimization of an incoherently pumped high-power random fiber laser," Photon. Res. **7**, 977 (2019).